Article

Large-Scale Meteorological Drivers of Extreme Precipitation Event and Devastating Floods of Early February 2021 in Semarang, Indonesia

Eddy Hermawan [1], Sandro W. Lubis [1,2], Teguh Harjana [1], Anis Purwaningsih [1], Risyanto [1,], Ainur Ridho [3], Dita Fatria Andarini [1], Dian Nur Ratri [4,5], Retno Widyaningsih [4]

1 National Research and Innovation Agency, Jakarta, Indonesia
2 Rice University, Houston, USA
3 Cerdas Antisipasi Risiko Bencana Indonesia (CARI), Indonesia
4 Meteorological, Climatological, and Geophysical Agency, Jakarta, Indonesia
5 Wageningen University and Research, Netherlands
* Correspondence: eddy001@brin.go.id
† Current address: National Research and Innovation Agency, Jakarta, Indonesia

Abstract: Unusually long duration and heavy rainfall on 5-6 February 2021 causes devastating floods in Semarang. The heavy rainfall is produced by two mesoscale convective systems (MCSs). The first MCS develops at 13Z on 5 February 2021 over the southern coast of Sumatra and propagates towards Semarang. The second MCS develops over the north coast of Semarang at 18Z on 5 February 2021, which later led to the first peak of precipitation at 21Z on 5 February 2021. These two MCSs eventually merge into single MCS, producing the second peak of precipitation at 00Z on 6 February 2021. Analysis of moisture transport indicates that the strong and persistent northwesterly wind near the surface induced by CENS prior to and during the event, creates an intensive meridional (southward) tropospheric moisture transport from the South China Sea towards Semarang. In addition, the westerly flow induced by low-frequency variability associated with La-Nina and the tropical depression associated with tropical cyclone formation over the North of Australia, produces an intensive zonal (eastward) tropospheric moisture transport from the Indian Ocean towards Semarang. The combined effects of the zonal and meridional moisture transports provide favorable conditions for the development of MCSs, and hence, extreme rainfall over Semarang.

Keywords: extreme precipitation; flood; cens; low-frequency variability, tropical depression, Semarang

Citation: Title. *Atmosphere* **2022**, *1*, 0. https://doi.org/

Received:
Accepted:
Published:

Publisher's Note: MDPI stays neutral with regard to jurisdictional claims in published maps and institutional affiliations.

1. Introduction

Semarang, the capital of Central Java province and one of the largest cities in Indonesia, is prone to damaging flooding due to tidal flooding from the sea and flash floods from the upper inland area [1]. This city is located on the northern coast of Java Island at 6°58S 110°25E (Figure 1). On Saturday, 6 February 2021, the city was hit by the flash floods triggered by extreme rainfall that inundated Semarang City and various areas of 10 subdistricts from Friday to Saturday [2]. According to the Agency for Meteorology, Climatology, and Geophysics (BMKG), the daily extreme rainfall intensity on 5 February 2021 was recorded up to 163.7 mm and 183 mm at the Klimatologi and Beringin Asri local weather stations, respectively. The flash floods triggered by this extreme rainfall is one of the most damaging flood events in the last ten years. It is estimated that 972 residents were evacuated from their homes, and many more reported severe property damages[3].

Previous studies have investigated atmospheric mechanisms driving of several flash floods in Semarang. Gernowo *et al.* [4] show that strong convection that produces a convective cloud (Cumulonimbus) triggers heavy rainfall and floods in Semarang in January 2013 and July 2016. Similarly, Faridatussafura and Wandala [5] using a weather forecast model with different convective and microphysics schemes find the same driving mechanism for the heavy rainfall in Semarang on 15 January 2013. Nonetheless, the role of large-scale meteorological drivers for the flash flood and extreme precipitation in Semarang is not well understood and has been rarely studied.

Extreme rainfall events that lead to flash floods are often associated with mesoscale convective systems (MCSs) [6–8]. Nuryanto *et al.* [9] studied MCSs over Jakarta by focusing on the distribution of MCSs using satellite data. They found that temporal variability of the MCS is often associated with a flood-producing storm. Furthermore, extreme precipitation over the northern part of Java and Java Island has also been linked to large-scale atmospheric variability from weekly to inter-seasonal timescales, such as Cold Surge (CS) and Cross Equatorial Northerly Surge (CENS) [10–12] and Madden Julian Oscillation (MJO) [13–15]. More recently, studies have found that equatorially trapped waves, including Kelvin waves, tropical-depression (TD)-type waves, eastward Inertio-Gravity (EIG) waves, mixed Rossby-Gravity (MRG) waves, and equatorial Rossby waves play a major role in organizing tropical convection and triggering floods[16–19]. In particular, Lubis and Respati [17] show that the convectively active phases of Kelvin waves can increase the probability of extreme rainfall over Java by up to 30%-60%.

In this study, we investigate the atmospheric driving mechanisms of the extreme rainfall and floods in Semarang on 5–6 February 2021. We focus on the effects of large-scale meteorological phenomena, including CENS, low-frequency variability, and tropical depression, that support the development of deep convection and heavy rainfall, by using in situ data, reanalysis, and satellite data. In addition, moisture transport and sources for extreme precipitation over Semarang on 5-6 February 2021 remain uncertain. Here, a backward tracking simulation using the HYSPLIT model is performed to search the moisture transport associated with the extreme rainfall event. The materials and methods of the study is further described in Section 2. In Section 3 we present the results and discussion. Furthermore, this is followed by the conclusions and future works in Section 4.

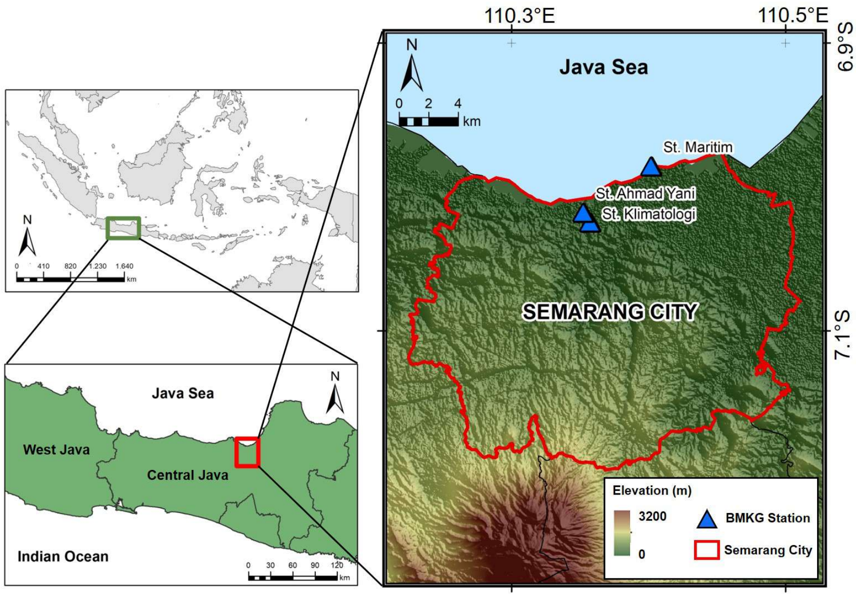

Figure 1. Area study of Semarang, located in Central Java province of Indonesia. The blue triangle is the rain gauge station used in this study. The color shading shows topography profile. The red line is administration boundary of Semarang.

2. Materials and Methods

2.1. *In situ data and ERA5*

The observational data used in this study include in-situ hourly measured rainfall data of high-resolution rain-gauge observation data operated by Meteorology, Climatology, and Geophysics Agency (BMKG). The data for the period of 5 February 2021 14Z to 6 February 2021 07Z are collected from three different local weather stations in Semarang, namely Maritime station, Ahmad Yani station, and Climatology Station (Figure 1 and see Supplementary Table S1).

In addition to in-situ observation data, this study also uses the fifth generation European Centre for Medium-Range Weather Forecasts (ECMWF) atmospheric reanalysis of the global climate (ERA5) [20]. The parameters used in this study include all parameters on single surface levels and pressure levels on a 0.25° × 0.25° latitude-longitude grid. The ERA5 is used as the input data for the Hybrid Single-Particle Lagrangian Integrated Trajectory (HYSPLIT) model in order to track the moisture source of heavy precipitation. Table 1 describes the parameters needed by the HYSPLIT model as the input data on pressure level and surface data, from 1 to 6 February 2021. These data were accessed from Copernicus Climate Change Service Climate Data Store (https://cds.climate.copernicus.eu/). The original data was in GRIB format data then it was converted into ARL format data that was adjusted with the HYSPLIT configuration.

Furthermore, the horizontal wind, mean sea level pressure, and potential vorticity parameters obtained from hourly temporal resolution at 925 hPa and 850 hPa pressure levels at the same period are also used to analyze CS, CENS, equatorial waves, and synoptic analysis.

Table 1. ERA5 parameters for HYSPLIT input data

	Data on pressure level	**Surface data**
Parameters	Temperature (K) Zonal component of wind (m/s) Meridional component of wind (m/s) Vertical velocity (Pa/s) Relative humidity (%) Specific humidity (kg/kg) Geopotential height (m) Potential vorticity (Km^2/kgs)	2m temperature (K) Surface pressure (hPa) Sea surface temperature (K)

2.2. *Satellite Data*

This study uses Himawari-8 satellite top brightness temperature (TBB) data at 10.4 μm infrared channel (Band 13) to identify the MCS, obtained from the Himawari Cast receiver operated by the National Agency of Research and Innovation (BRIN) installed at Bandung, Indonesia. The data have a spatial resolution of 4x4 km and an hourly temporal resolution to track the movement of the convective clouds. The Advance Himawari Imager (AHI), the only payload onboard the satellite, has a capability to cover the Asia Pacific and Australia regions, including Indonesia with up to every 10-minutes near real-time observation [21]. This allows us to monitor the clouds' movement and their growth. The 10.4 μm channel detects the surface body temperature of the Earth. In addition, the Global Satellite Mapping of Precipitation (GSMaP) gauge-corrected version-7 standard precipitation product is also used in this study to investigate the spatial distribution of rainfall associated with the MCS. We use an hourly rain rate with a horizontal resolution of 0.1x0.1 degree (https://sharaku.eorc.jaxa.jp/GSMaP/).

2.3. Sea Surface Temperature Data

Sea surface temperature (SST) daily anomaly data were retrieved from NOAA high-resolution blended analysis of daily SST and ice dataset [22] on a 0.25° × 0.25° latitude-longitude grid for the period of 4 to 6 February 2021.

2.4. MCS Identification

Identification of the MCS in this study is based on the "Grab 'em, Tag 'em, Graph 'em" (GTG) algorithm [23]. The method has been applied to previous studies of MCSs in Indonesia [24] as well as for analysing heavy precipitation events in Jakarta [9][25]. The GTG algorithm can resolve the issue related to the complex evolution of MCS [23] as it allows multiple convective cells to merge simultaneously to form a larger convective system. MCS is defined by the convective cloud cluster, which has to meet some criteria as described in Table 2. The detailed description of the GTG algorithm can be found in[23] [24].

Table 2. Criteria of MCS defined in this study

Physical Characteristics	
(BT10.4)	243 K
Size	10,000 km^2
Duration	Size and temperature definition must be met for a period of 3 hours
Initiation	Size and temperature definition are first satisfied
Termination	Size and temperature definition are no longer satisfied
Mature	Minimum mean of cloud temperature definition must be met

2.5. HYSPLIT Model and Backward Trajectories

The HYSPLIT model version 5.1 developed by Air Resources Laboratory (ARL), The National Oceanic and Atmospheric Administration (NOAA) [26,27] is used to calculate backward trajectories of moisture and its complex transport. This model combines a hybrid of Lagrangian and Eulerian methodology. However, because in this study we tracked a moving air parcel by considering the advection calculations, so we only applied the Lagrangian model. We track the moisture source and transport that lead to high precipitation amounts over Semarang during the flood event on 5-6 February 2021. This Lagrangian approach considers advection calculation as the trajectory of the parcel air moving from the initial place. The trajectory is determined by the calculation of the new position at a time step (t+ Δ t) as a result of wind advection. The change in the position air parcel vector with time is calculated from the average velocity vectors at their initial and first-guess positions [28].

We run the model for 35 different locations in Semarang (between 6.89-7.49°S and 110.22-110.62°E) at two peaks of precipitation events during the Semarang flood; the first peak is at 5 February 2021 at 21Z and the second peak is at 6 February 2021 at 00Z. We run the model to generate 72 hours backwards trajectories. Furthermore, to better understand the source of the moisture transport as a function of height, we run the model on three different atmospheric layers; (1) lower layer ($850 \leq p \leq 1000$) hPa, (2) middle layer ($700 \leq p < 850$) hPa and (3) the upper layer ($100 < p < 700$) hPa. As we will show the letter in the "Result Section", the transport of moisture that causes heavy rainfall over Semarang are driven by the different phenomenon that is dominant at certain atmospheric layers.

2.6. *Water Vapor Transport and Moisture Flux convergence*

The integrated vertical water vapour transport (IVT) and vertically integrated moisture flux convergence (VIMFC) are calculated for the three different atmospheric layers (lower layer ($850 \leq p \leq 1000$) hPa, middle layer ($700 \leq p < 850$) hPa and upper layer ($100 < p < 700$)hPa) using these following equations [17,18,29]:

$$\mathrm{IVT} = \left[\left(\frac{1}{g} \int_b^a qu \, \mathrm{d}p \right)^2 + \left(\frac{1}{g} \int_b^a qv \, \mathrm{d}p \right)^2 \right]^{1/2}, \tag{1}$$

$$\mathrm{VIMFC} = \frac{-1}{g} \int_b^a \left(\frac{\partial uq}{\partial x} + \frac{\partial vq}{\partial y} \right) dp, \tag{2}$$

where u and v represent zonal and meridional wind velocity (m/s), q is specific humidity (g/kg), p is pressure (Pa), a is the upper limit of each layer, and b is bottom limit of each layer.

2.7. *CENS and CS Indices*

The Cross equatorial northerly surge (CENS) index is defined as an area-averaged of near-surface level meridional wind magnitude over 105°-115°E and 0°-5°S Hattori *et al.* [30]. The active phase of CENS is signified by its value exceeding 5 m/s, indicating strengthening northerly flow over the Java Sea. Furthermore, cold surge (CS) is defined as an areal averaged of meridional wind at 925 hPa between 110°–117.5°E, 15°N exceeding 8 m/s [31].

3. Results

3.1. *Characteristics of Extreme Rainfall*

On February 5, 2021, prolonged heavy rainfall occurred in Semarang from 16Z to 00Z. The highest mean rainfall intensity was recorded at 21Z of up to 48 mm.hr^{-1} (averaged over 3 rain gauge stations) and followed by the second peak up to 32 mm.hr^{-1} at 00Z on 6 February 2021 (Figure 2). Heavy rains continue until 06Z and start to decrease thereafter. The total amount of precipitation from 16Z 5 February to 06Z 6 February reaches up to 218 mm.hr^{-1}, which meets the definition of extreme rainfall by BMKG, where the accumulated rainfall is more than 150 mm within a 24-hour period.

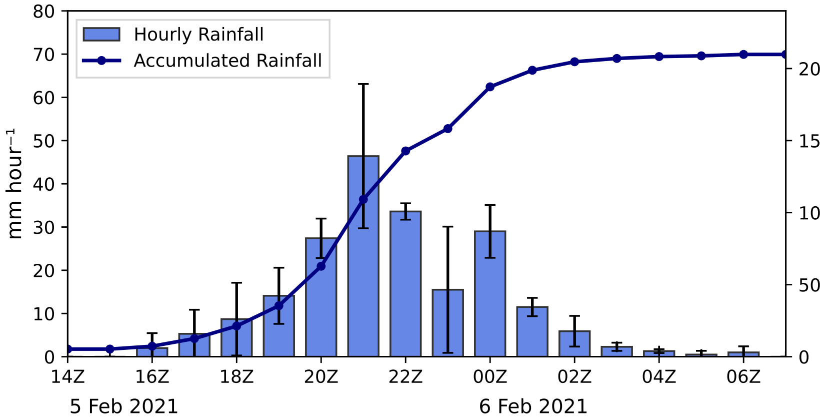

Figure 2. Time series of hourly rainfall averaged from 3 rain gauge stations. The vertical line indicate with a standard deviation and the contour line indicates accumulated precipitation from 00Z 5 February to 07Z 6 February 2021.

3.2. Evolution of Mesoscale Convective System (MCS)

Figure 3 shows the three-hourly evolution of MCS during the period of heavy rainfall (see Supplementary Figure S1 for a hourly evolution of MCS). Two MCSs were identified prior to and during the occurrence of heavy rainfall, which triggered the flood event in Semarang on 6 February 2021. The first MCS was developed over the southern coast of Sumatra and initiated at 13Z on 5 February 2021. The size of this cloud cluster is 8,704 km^2 and grew steadily until reached a size of 23,552 km^2 after two hours (Figure 3b). The second MCS develops over the western area of Semarang at 18Z on 5 February 2021. While the first MCS propagate eastward towards Semarang, the second MCS grows and becomes more mature, resulting in heavy precipitation over the region at 21Z on 5 February 2021 (Figure 3c). Therefore, the first peak of rainfall in Semarang is associated with the local development of the second MCS (Figure 3d). At 00Z on 6 February 2021, the second MCS eventually merges with the first MCS after three hours (Figure 3e), resulting in one deep MCS. This MCS in its mature stage is responsible for the increased precipitation at 00Z on 6 February 2021, marking the second peak of precipitation. Thereafter the MCS gradually dissipates, followed by decreasing in rainfall intensity. In general, the spatial evolution of rain rates from GSMaP is consistent with the development of MCSs, suggesting that they play an important role in the formation of extreme rainfall over the region.

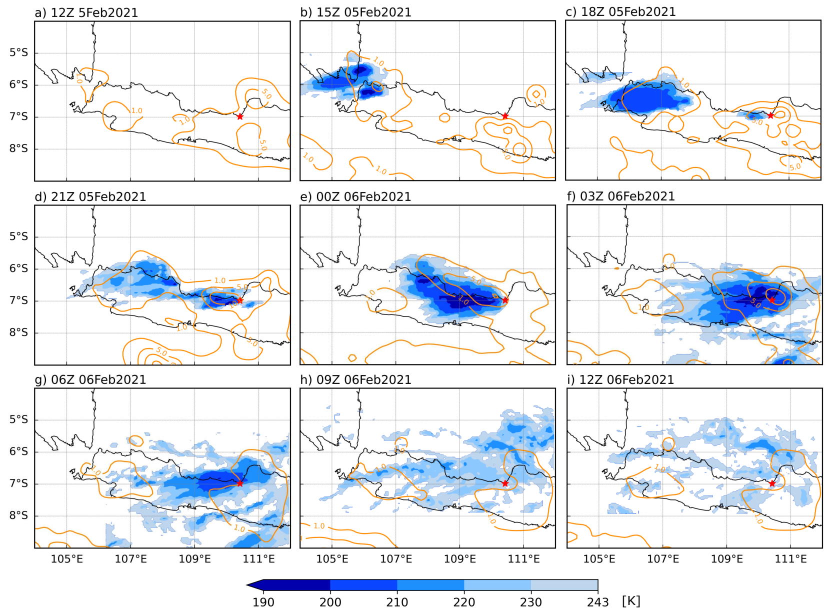

Figure 3. Three-hourly evolution of the MCS (K, shaded) from Himawari-8 satellite superimposed with rainfall rate from GSMaP ($mm.hr^{-1}$, contour) for the period of 5 February at 12Z to 6 February 2021 at 12Z. The location of Semarang is denoted by a red star.

3.3. Moisture Sources and Transport for Extreme Precipitation

Our results so far indicate that two MCS initially identified the southern coast of Sumatra and the western area of Semarang (Figure 3) is responsible for the extreme rainfall over Semarang. Previous studies show that initiation and development of MCS that result in heavy precipitation are associated with higher moisture supply [32]. Here, we analyse the moisture supply that supports the development of these MCSs for the period of 72-h prior to the peaks of precipitation.

To determine the sources of moisture for the devastating precipitation event in Semarang in early February 2021, moisture transport is tracked back using a Lagrangian approach with HYSPLIT model at the two rainfall peaks (i.e., 21Z on 5 February 2021 and 00Z on 6 February 2021). In general, the moisture transport towards the flooding region can be grouped into three clusters: the bottom/near surface layer ($850 \leq p \leq 1000$) hPa, the middle layer ($700 \leq p < 850$) hPa, and the upper layer ($100 < p < 700$) hPa. Figure 4 shows the backward trajectories of moisture calculated for each layer defined above. In the upper layer, the moisture transport over Semarang is mostly dominated by the zonal transport originating from the Indian Ocean (Figure 4a-b). In the middle layer, enhanced moisture over Semarang is a combination of the meridional transport from the South China Sea and the zonal transport from the Indian Ocean (Fig. 4c-d). Tracking over the bottom layer indicates that moisture is transported from the South China Sea towards Semarang (Figure 4e-f). In particular, the specific humidity (Q) along pathways is considerably higher (around 16-18 gr/kg) over the MCS formation location (Figures 4e,f). Moreover, moisture content over the middle and upper layers is quite comparable.

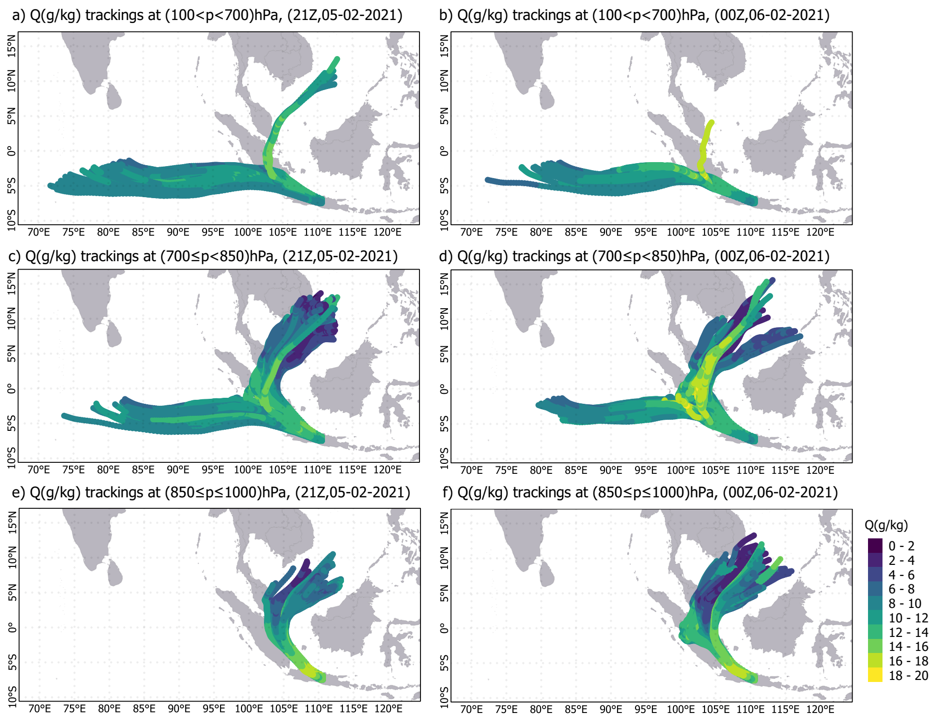

Figure 4. Characteristics of moisture transport prior to and during the period of maximum precipitation events in Semarang. The 72-hr backward moisture trajectories (lines) of the two peaks of precipitation events: (a, c, e) 21Z 05 February 2021 and (b, d, f) 00Z 06 February 2021 are shown at the three different layers: (a)-(b) ($100 < p < 700$) hPa, (c)-(d) ($700 \leq p < 850$) hPa, and (e)-(f) ($850 \leq p \leq 1000$) hPa. Colors on the pathways indicate the average specific humidity of air parcels along the trajectories (g/kg).

The results of the trajectory analysis above are consistent with the Eulerian approach based on IVT analysis. Figure 5 shows the time-integrated IVT for 72-h prior to the period of maximum precipitation events at these three layers. it is evident that the water vapour is more abundant in the bottom layer than in the other two layers. In this layer, the highest moisture content (more than 700 10^{-5} kg.m^{-1} in three days) can be found over oceans around Java Island and over the South China Sea (Fig. 5e,f). Moreover, moisture content over the middle and upper layers is quite comparable, with the highest moisture transport (400-600 10^{-5} kg.m^{-1} within 3 days) over Java Island and its surroundings (Figs. 5a-d).

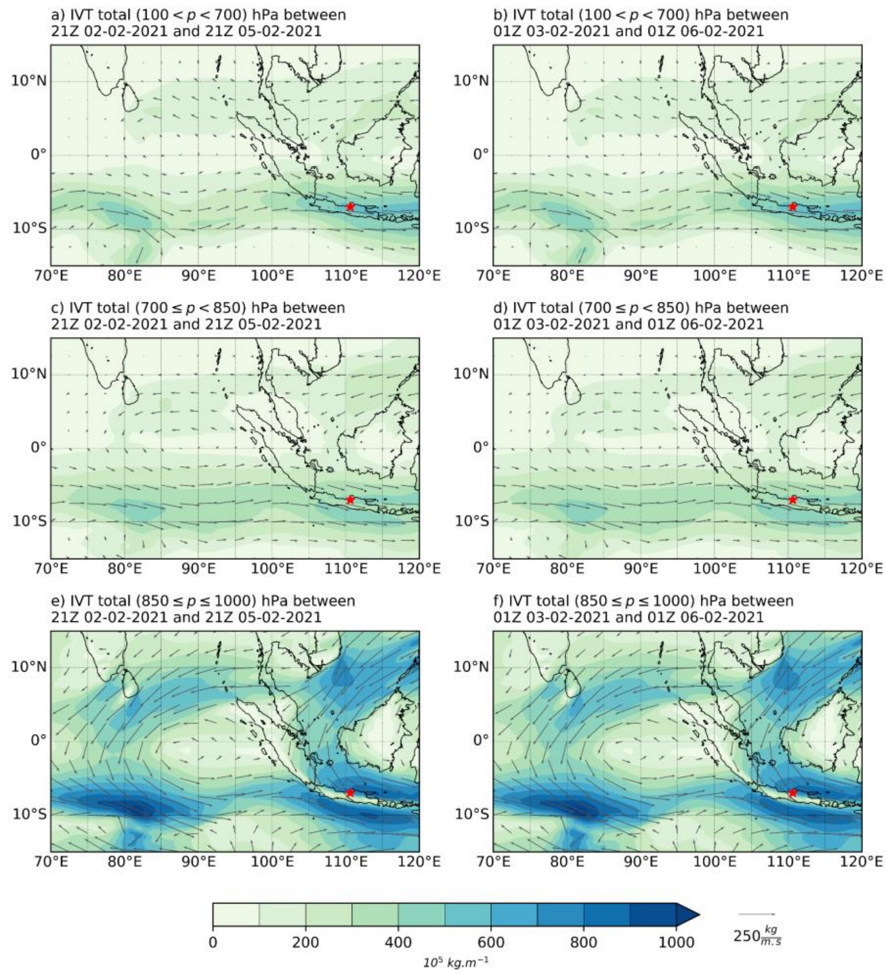

Figure 5. Time-integrated IVT for 72-h prior to the period of maximum precipitation events: (a, c, e) 21Z 02 to 21Z 05 February 2021 and (b, d, f) 00Z 03 - 00Z 06 February 2021 over three different layers: (a)-(b) (100 $< p <$ 700) hPa, (c)-(d) (700 $\leq p <$ 850) hPa, and (e)-(f) (850 $\leq p \leq$ 1000) hPa.

The enhanced moisture transport can lead to an increase in precipitation because of the convergence of the moisture flux [17,18]. Figure 6 shows the hourly time evolution of the vertically integrated moisture flux convergence (VIMFC) over Semarang, similar to Figure 2. It is evident that the time evolution of precipitation during the period of heavy rainfall over Semarang (Fig. 2) can be explained by the time evolution of VIMFC. This suggests that the enhanced moisture transport towards Semarang leads to increased precipitation through the convergence of the moisture fluxes (Fig. 6a). Furthermore, by decomposing the VIMFC into three layers, it is evident that the first peak of rainfall (21Z, 5 February 2021) is mainly attributed to the enhanced VIMFC on the bottom layer (Fig. 6b), while the second rainfall peak (00Z, 06 February 2021) is dominated by the moisture in the middle layer (Fig. 6b).

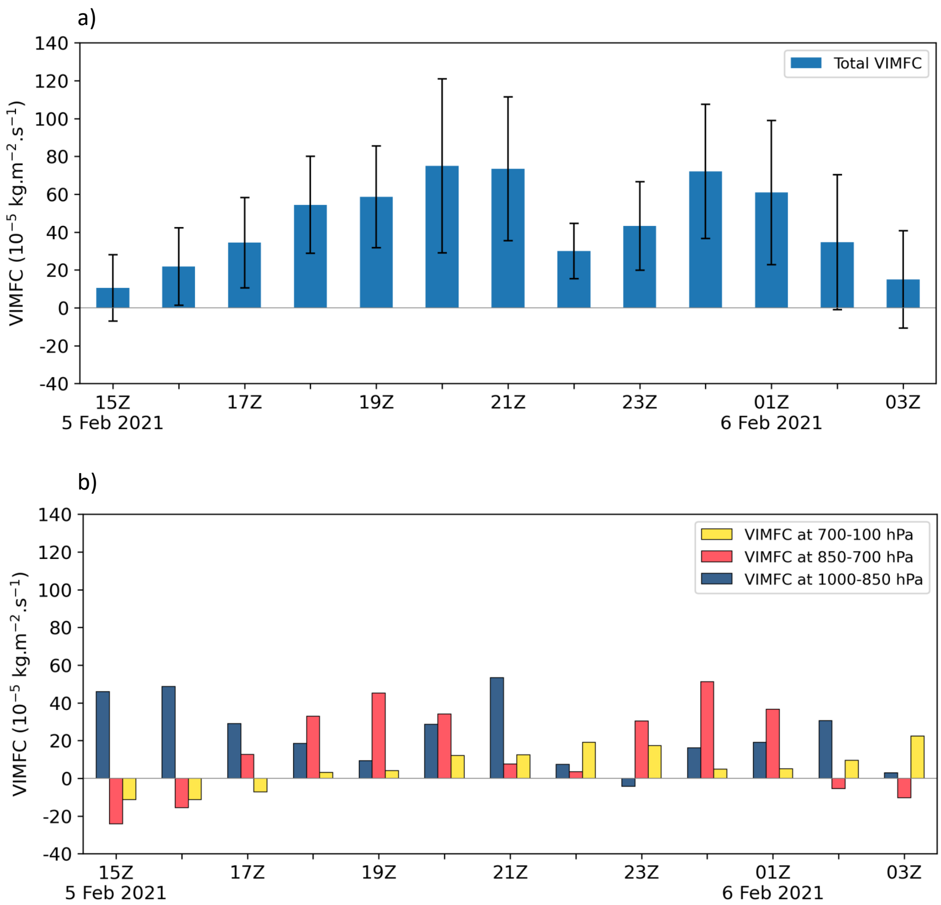

Figure 6. Hourly time evolution of the vertically integrated moisture flux convergence (VIMFC, 10^{-5} kg.m^{-2}.s^{-1}) over the Greater Semarang area calculated for (a) the total atmospheric columns with its standard deviation, and (b) the three layers defined in the study i.e. upper-layer ($100 < p < 700$) hPa; middle-layer ($700 \leq p < 850$) hPa; and bottom-layer ($850 \leq p \leq 1000$) hPa during 15Z 5 February 2021 – 03Z 6 February 2021

Our results above indicate that zonal (eastward) and meridional (southward) transport of moisture towards Semarang play important role in the development MCS and the extreme rainfall (Fig. 4 and 5). It is also shown that enhanced moisture transport can lead to an increase in precipitation because of the convergence of the moisture/water vapour fluxes (Fig. 6). The question now is what the mechanisms driving of such transport. As seen in Fig. (4e,f) and (Figure 5e,f), the cross-equatorial moisture transport is detected at the bottom and middle layers from both trajectory and IVT analysis. This near surface meridional transport of moisture is consistent with the strong northerly moisture transported from the South China Sea towards the northern part of Java Island (vector in Figure 5e,f). Several studies have shown that moisture transported from this area contributes to the enhancement of rainfall over the northern part of Java Island [30,33], which is correlated with CENS and CS. Therefore the northerly moisture transport in the Semarang flood is suspected to be associated with CENS (see subsection 3.4.1 for further discussion). Furthermore, the zonal moisture transport is also responsible for the additional moisture supply. The moisture is advected from the Indian Ocean at the middle and upper layers of Semarang (Figure 4a-d). The zonal transport of moisture is suspected to be associated with zonal circulation associated with the active phase of La-Nina and tropical depression (TD) due to TC formation over the North of Australia (see subsection 3.4.2 for further discussion).

3.4. Large-Scale Atmospheric Circulation Responsible for Extreme Precipitation

In this section, we will investigate the mechanisms responsible for driving of such zonal and meridional moisture transport towards Semarang. Here, we focus on the role of large-scale atmospheric drivers such as CENS, low-frequency variability, and synoptic activity during the period of the extreme rainfall.

3.4.1. The Role of Cross Equatorial Northerly Surge (CENS)

Figure 7 shows the time evolution of CENS from 12Z 2 February to 03Z 7 February 2021. It is evident that a strong and persistent CENS has started on 21Z 2 February 2021 with the amplitude between -7 m/s to -5 m/s. The occurrence of the CENS is preceded by CS due to the cold temperature over the South China Sea (see later in Fig. 9). This indicates that the strengthening of the near surface meridional wind (at 925 hPa) from the South China Sea all the way to Semarang is associated with CENS. On 21Z 5 February 2021, CENS reaches its maximum strength and the rainfall reached the first and second of peaks rainfall intensity. Although the prevailing monsoon wind pattern is already formed prior to the extreme rainfall event, however, its strength is relatively weak and has not yet reached the northern coast of Central Java. Therefore, the strong northerly moisture transported from the South China Sea towards the northern part of Java Island (as shown in the bottom and middle layers of moisture transports/trajectories in Figs. 5 and 6) is associated with strong and persistent CENS.

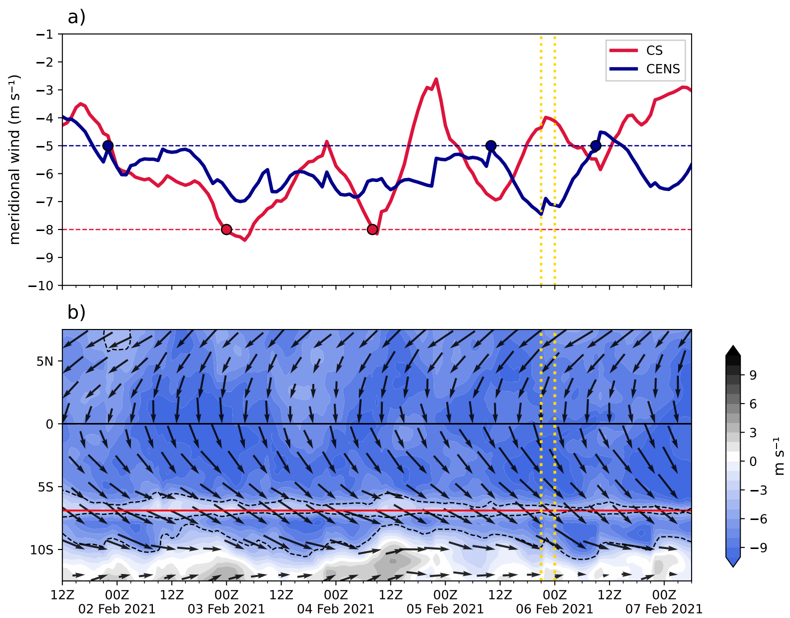

Figure 7. (**a**) Time series of cross equatorial northerly surge (CENS) (blue line) and cold surge (CS) (red line), the horizontal dash line indicates the threshold of an activated mode of CENS and CS. (**b**) Time-latitude of 925 hPa horizontal wind magnitude and direction (arrows), contour-fill represent of meridional wind and the dotted line shows the value of 5 m/s, the red line marked latitude of Semarang coastline, the vertical yellow line marked of rainfall peaks. Both a) and b) x-axis are span from 12Z 2 February to 03Z 7 February 2021.

3.4.2. The Role of Low-Frequency Variability and Tropical Depression

To understand the mechanisms that drive the zonal (eastward) transport of moisture towards Semarang prior to and during the extreme events, we analyze the daily evolution of zonal wind anomaly (color shading) and total wind anomaly (vectors) at 850 hPa. We decompose the wind anomalies into the contribution of MJO, low-frequency variability (>120 days) and the residual. It is evident that during the period of extreme precipitation, MJO does not contribute significantly to the zonal component of the wind (see vectors and color shading in Figs. 8a,d.

On the other hand, low-frequency variability has a greater contribution to strengthening the westerly wind in the Java Island and area around Semarang (Figs. 8b,e). The active La-Nina causes a stronger zonal wind circulation especially over the southern part of the maritime continent region due to the formation of the warm pool over the West Pacific (see also Fig. 9a). The water vapour content transported by this westerly wind explains the source of moisture from the Indian Ocean heading to the Semarang. In addition, the low-frequency variability also plays a role in strengthening the north-westerly flow that brings moisture towards Semarang.

Another driving factor that supports the zonal transport of moisture from the Indian Ocean heading to the Semarang is the zonal circulation driven by synoptic activity associated with the tropical depression over the North of Australia. It can be seen that the residual anomaly in Fig. 8 is mainly associated with this phenomenon with a time scale of less than 30 days (Figs. 8c,f). This tropical depression associated with the formation of tropical cyclone, causes a fairly strong air pressure gradient and attracts the moisture flowing from the west to the east.

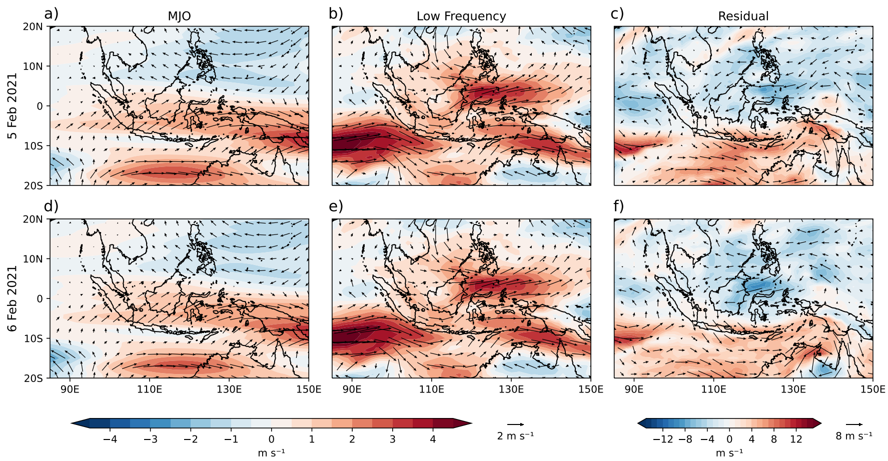

Figure 8. Daily evolution of 850 hPa zonal wind (color shading) and total wind anomalies (vector) anomalies during the Semarang flood event. Wind anomalies filtered for (a) Madden–Julian oscillation (MJO), (b) the low-frequency oscillation (> 120 days), and (c) residuals (total - (MJO+low frequency)). Note that the amplitude used for the residuals is different 5from MJO and low-frequency variability.

Finally, the influence of the CENS, low-frequency variability, and tropical depression on the moisture transports is consistent with the background SST condition during the period of extreme rainfall in Semarang (Fig. 9a). Colder SST anomalies were observed in the South China Sea region lower to -2°C and the Indian Ocean region to the west of Java Island lower to -1°C. Meanwhile, positive anomalies are seen in the seas of the Maritime Continent to the east and in the south of Java, with an anomaly of 2°C spreading extensively. The meridional SST gradient between the South China Sea region and Java drive the development of CENS. On the other hands, the zonal SST gradient between the Indian Ocean and West Pacific warm pool drive the zonal circulation associated with low-frequency variability (La-Nina). In addition, the formation of tropical depression over the North of Australia is consistent with the high positive potential vorticity and low-pressure anomalies (Fig. 9b). This low-pressure system associated with the tropical depression is also likely responsible to strengthen zonal wind from the Indian Ocean towards Semarang.

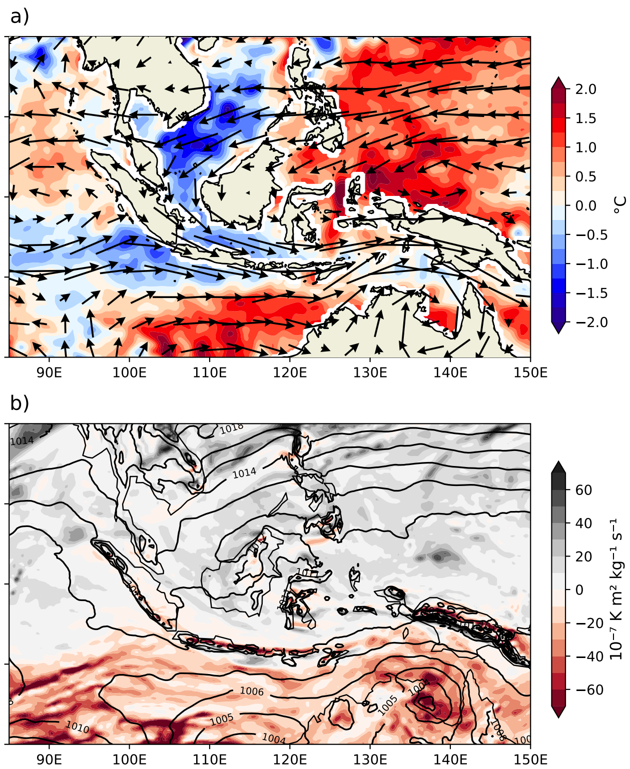

Figure 9. (**a**) SST anomalies superimposed with 850 hPa horizontal wind anomalies (vectors) averaged from 4 to 6 February 2021. (**b**) 850 hPa potential vorticity (PV) anomalies superimposed with mean sea level pressure anomalies averaged from 4 to 6 February 2021.

4. Conclusion and Discussion

This study investigates the mechanisms driving the extreme precipitation events produced by two MCSs during the devastating flood event in Semarang on 5–6 February 2021, using ERA5 reanalysis, satellite data, and in-situ data. The key findings of our results can be summarized as follow:

- There are three large-scale meteorological drivers that contribute to the flooding event triggered by the extreme rainfall over Semarang, namely, CENS, low-frequency variability associated with La-Nina, and tropical depression over the North of Australia.
- A strong and persistent CENS prior to and during the extreme event contribute significantly to the deep convection over the Semarang. CENS drives the meridional (southward) low-level transport of moist air from the South China Sea towards the northern part of Java Island, supporting the development of the two MCSs that produces extreme precipitation over Semarang.
- Low-frequency variability associated with La Nina and the synoptic activity associated with the tropical depression together contribute to development of the zonal propagation of MCS and the enhanced moisture over Semarang. Both of them play an important role in the eastward transport of moist air from the Indian Ocean to Semarang.

The main results above can be also summarized in a conceptual diagram in Figure 10. The diagram illustrates that the influence of CENS is dominant at the bottom/near surface layer ($850 \leq p \leq 1000$) hPa and partly at the middle layer ($700 \leq p < 850$) hPa. The effects of La Nina transport moisture from the Indian Ocean to Semarang is mainly in the upper layer ($100 < p < 700$) hPa. In addition, a low pressure located in the north of Australia associated with a tropical depression strengthens the westerly winds to supply the moisture in the MCS development over the region.

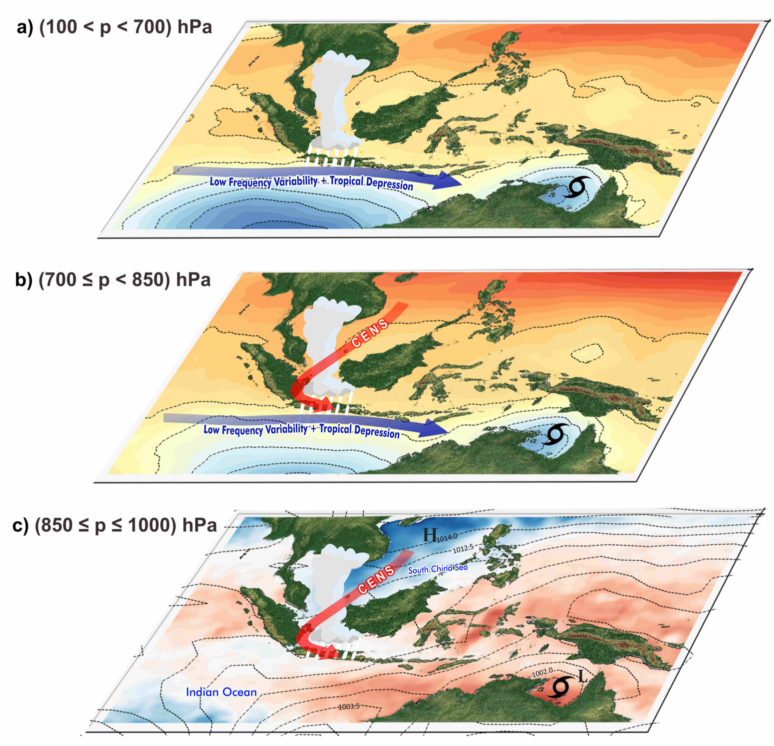

Figure 10. A schematic diagram of large-scale meteorological drivers behind extreme precipitation during the Semarang Flood Event, 5 - 6 February 2021 at (**a**) ($100 < p < 700$) hPa, (**b**) ($700 \leq p < 850$) hPa, and (**c**) ($850 \leq p \leq 1000$) hPa.

Previous studies have revealed that CENS is a prominent feature in the MCS development over the tropical region and enhances the convective activities over the Java Sea and the northern part of Java Island [25,30]. However, it is not yet known to what extent CENS can exert its influence further to the east of the north coast of Java Island. Since the north coast of Central Java is located slightly further south than the north coast of West Java, there must be very strong and persistent northerly winds to have significant influence on Central Java. This is the case here for the extreme rainfall in Semarang, in which northerly winds are observed in a very strong and persistently condition of up to 3 days in the Java Sea before the event takes place. In addition, in this particular flooding case, both westerly and northerly winds persistently transport the moisture from the Indian Ocean and the South China Sea and altogether creating favorable deep convective environment for development of MCSs and hence, extreme rainfall over the region.

This is the first study to demonstrate the role of large-scale meteorological drivers for the extreme precipitation that caused the widespread flooding in Semarang on 5-6 February 2021. It is possible that other roles of large-scale atmospheric phenomena can also initiate the occurrences of extreme precipitation in other major flood cases in Semarang, such as Indian Ocean Dipole (IOD) [34,35] and equatorial waves [16–18,36], though they are not the case in our case study. In addition, the unique interaction between those atmospheric variability and local effects or topography and ocean could also affect the extreme precipitation.

Overall, our study suggests that the intensive low-level wind induced by CENS and the westerly flow modulated by the La Nina circulation and tropical depression are the main meteorological factors that produced unusual heavy rainfall during the flood event in Semarang on 5-6 February 2021. The result of this study would improve our understanding of the atmospheric driving mechanisms of extreme precipitation, especially in Semarang, Central Java, Indonesia.

Author Contributions: E.H., S.L., and T.H. are the main contributors. Conceptualization, S.L. and E.H.; methodology, S.L., A.P., R.R., A.R., and D.A.; software, A.R., A.P., and R.R.; validation, A.R.; formal analysis, S.L., A.P., R.R., A.R., and D.A; Data, R.W., A.P., R.R., A.R., and D.A writing—original draft preparation, D.R., A.P., R.R., A.R., and D.A; writing—review and editing, S.L. and D.R.; visualization, A.P., R.R., A.R., and D.A; funding acquisition, E. H. All authors have read and agreed to the published version of the manuscript.

Funding: This research was funded by the Budget Execution (Allotment) Document, National Research and Innovation Agency (BRIN) 2022 (grant no. SP DIPA-124.01.1.690504/2022).

Institutional Review Board Statement: No applicable.

Informed Consent Statement: No applicable.

Data Availability Statement: The ERA-5 meteorological reanalysis dataset used in this study is available from the European Centre for Medium-Range Weather Forecasts (https://www.ecmwf.int/en/forecasts/datasets/reanalysis-datasets/era5). The SST data is publicly available online at the NOAA web page (https://psl.noaa.gov/data/gridded/data.ncep.reanalysis2.html). The hourly rainfall data from the Global Satellite Mapping of Precipitation (GSMaP) can be accessed freely through https://sharaku.eorc.jaxa.jp/GSMaP/. The Himawari-8 satellite top brightness temperature (TBB) data and in-situ hourly rainfall data presented in this study are available upon request from the corresponding authors.

Acknowledgments: The authors would like to thank all the staff at the Meteorological Station in Semarang for providing the in-situ observational data for this study

Conflicts of Interest: The authors declare no conflict of interest.

Sample Availability: No applicable

References

1. Marfai, M.A.; King, L. Coastal flood management in Semarang, Indonesia. *Environmental geology* **2008**, *55*, 1507–1518.
2. antaranews.com. Semarang's flooding caused by extreme rainfall, tidal flooding: govt - ANTARA News — en.antaranews.com. https://en.antaranews.com/news/167488/semarangs-flooding-caused-by-extreme-rainfall-tidal-flooding-govt. [Accessed 04-Jun-2022].
3. Flood in Semarang and three alternative solutions — flows.hypotheses.org. https://flows.hypotheses.org/6071. [Accessed 03-Jun-2022].
4. Gernowo, R.; Adi, K.; Yulianto, T.; Seniyatis, S.; Yatunnisa, A. Hazard mitigation with cloud model based rainfall and convective data. *Journal of Physics: Conference Series* **2018**, *1025*, 012023. doi:10.1088/1742-6596/1025/1/012023.
5. Faridatussafura, N.; Wandala, A. Convective and microphysics parameterization impact on simulating heavy rainfall in Semarang (case study on February 12supth/sup, 2015). *Journal of Physics: Conference Series* **2018**, *1025*, 012027. doi:10.1088/1742-6596/1025/1/012027.
6. Doswell III, C.A. Seeing supercells as heavy rain producers. Preprints, 14th Conf. on Hydrology, Dallas, TX, Amer. Meteor. Soc, 1998, pp. 73–79.
7. Schumacher, R.S.; Johnson, R.H. Mesoscale processes contributing to extreme rainfall in a midlatitude warm-season flash flood. *Monthly Weather Review* **2008**, *136*, 3964–3986.
8. Hu, H.; Feng, Z.; Leung, L.Y.R. Linking flood frequency with mesoscale convective systems in the US. *Geophysical Research Letters* **2021**, *48*, e2021GL092546.
9. Nuryanto, D.E.; Pawitan, H.; Hidayat, R.; Aldrian, E. The occurrence of the typical mesoscale convective system with a flood-producing storm in the wet season over the Greater Jakarta area. *Dynamics of Atmospheres and Oceans* **2021**, *96*, 101246.
10. Wu, P.; Hara, M.; Fudeyasu, H.; Yamanaka, M.D.; Matsumoto, J.; Syamsudin, F.; Sulistyowati, R.; Djajadihardja, Y.S. The Impact of Trans-equatorial Monsoon Flow on the Formation of Repeated Torrential Rains over Java Island. *SOLA* **2007**, *3*, 93–96.
11. Trilaksono, N.J.; Otsuka, S.; Yoden, S.; Saito, K.; Hayashi, S. Dependence of Model-Simulated Heavy Rainfall on the Horizontal Resolution during the Jakarta Flood Event in January-February 2007. *SOLA* **2011**, *7*, 193–196.
12. Trilaksono, N.J.; Otsuka, S.; Yoden, S. A Time-Lagged Ensemble Simulation on the Modulation of Precipitation over West Java in January–February 2007. *Monthly Weather Review* **2012**, *140*, 601 – 616. doi:10.1175/MWR-D-11-00094.1.
13. Hidayat, R.; Kizu, S. Influence of the Madden–Julian Oscillation on Indonesian rainfall variability in austral summer. *International Journal of Climatology* **2010**, *30*, 1816–1825, [https://rmets.onlinelibrary.wiley.com/doi/pdf/10.1002/joc.2005]. doi:https://doi.org/10.1002/joc.2005.
14. Wu, P.; Arbain, A.A.; Mori, S.; Hamada, J.I.; Hattori, M.; Syamsudin, F.; Yamanaka, M.D. The Effects of an Active Phase of the Madden-Julian Oscillation on the Extreme Precipitation Event over Western Java Island in January 2013. *SOLA* **2013**, *9*, 79–83.

15. Muhammad, F.R.; Lubis, S.W.; Setiawan, S. Impacts of the Madden–Julian oscillation on precipitation extremes in Indonesia. *Int. J. Climatol.* **2021**, *41*, 1970–1984.
16. Lubis, S.W.; Jacobi, C. The modulating influence of convectively coupled equatorial waves (CCEWs) on the variability of tropical precipitation. *International Journal of Climatology* **2015**, *35*, 1465–1483. doi:https://doi.org/10.1002/joc.4069.
17. Lubis, S.W.; Respati, M.R. Impacts of convectively coupled equatorial waves on rainfall extremes in Java, Indonesia. *International Journal of Climatology* **2021**, *41*, 2418–2440.
18. Latos, B.; Lefort, T.; Flatau, M.K.; Flatau, P.J.; Permana, D.S.; Baranowski, D.B.; Paski, J.A.; Makmur, E.; Sulystyo, E.; Peyrillé, P.; et al. Equatorial waves triggering extreme rainfall and floods in southwest Sulawesi, Indonesia. *Monthly Weather Review* **2021**, *149*, 1381–1401.
19. Peatman, S.C.; Schwendike, J.; Birch, C.E.; Marsham, J.H.; Matthews, A.J.; Yang, G.Y. A local-to-large scale view of Maritime Continent rainfall: control by ENSO, MJO and equatorial waves. *Journal of Climate* **2021**, pp. 1 – 52. doi:10.1175/JCLI-D-21-0263.1.
20. Hersbach, H.; Bell, B.; Berrisford, P.; Hirahara, S.; Horányi, A.; Muñoz-Sabater, J.; Nicolas, J.; Peubey, C.; Radu, R.; Schepers, D.; et al. The ERA5 global reanalysis. *Quarterly Journal of the Royal Meteorological Society* **2020**, *146*, 1999–2049, [https://rmets.onlinelibrary.wiley.com/doi/pdf/10.1002/qj.3803]. doi:https://doi.org/10.1002/qj.3803.
21. Bessho, K.; Date, K.; Hayashi, M.; Ikeda, A.; Imai, T.; Inoue, H.; Kumagai, Y.; Miyakawa, T.; Murata, H.; Ohno, T.; et al. An Introduction to Himawari-8/9— Japan's New-Generation Geostationary Meteorological Satellites. *Journal of the Meteorological Society of Japan. Ser. II* **2016**, *94*, 151–183.
22. Huang, B., C.L.V.B.E.F.G.G.B.H.T.S.; Zhang, H.M. Improvements of the Daily Optimum Interpolation Sea Surface Temperature (DOISST) Version 2.1. *Journal of Climate* **2021**, *34*, 2923–2939.
23. Whitehall, K.; Mattmann, C.A.; Jenkins, G.; Rwebangira, M.; Demoz, B.; Waliser, D.; Kim, J.; Goodale, C.; Hart, A.; Ramirez, P.; et al. Exploring a graph theory based algorithm for automated identification and characterization of large mesoscale convective systems in satellite datasets. *Earth Sci. Inform.* **2015**, *8*, 663–675.
24. Putri, N.S.; Hayasaka, T.; Whitehall, K.D. The Properties of Mesoscale Convective Systems in Indonesia Detected Using the Grab 'Em Tag 'Em Graph 'Em (GTG) Algorithm. *Journal of the Meteorological Society of Japan. Ser. II* **2017**, *95*, 391–409.
25. Nuryanto, D.E.; Pawitan, H.; Hidayat, R.; Aldrian, E. Characteristics of two mesoscale convective systems (MCSs) over the Greater Jakarta: case of heavy rainfall period 15–18 January 2013. *Geoscience Letters* **2019**, *6*, 1.
26. Chock, D.P.; Winkler, S.L. A particle grid air quality modeling approach: 2. Coupling with chemistry. *J. Geophys. Res.* **1994b**, *99*, 1033–1041.
27. Stein, A.F.; Draxler, R.R.; Rolph, G.D.; Stunder, B.J.B.; Cohen, M.D.; Ngan, F. NOAA's HYSPLIT Atmospheric Transport and Dispersion Modeling System. *Bulletin of the American Meteorological Society* **2015**, *96*, 2059 – 2077. doi:10.1175/BAMS-D-14-00110.1.
28. Draxler, R.R.; Hess, G.D. An overview of the HYSPLIT_4 modelling system for trajectories, dispersion, and deposition. *Australian Meteorological Magazine* **1998**, *47*, 295–308.
29. van Zomeren, J.; van Delden, A. Vertically integrated moisture flux convergence as a predictor of thunderstorms. *Atmospheric Research* **2007**, *83*, 435–445. European Conference on Severe Storms 2004, doi:https://doi.org/10.1016/j.atmosres.2005.08.015.
30. Hattori, M.; Mori, S.; Matsumoto, J. The Cross-Equatorial Northerly Surge over the Maritime Continent and Its Relationship to Precipitation Patterns. *Journal of the Meteorological Society of Japan* **2011**, *89A*, 27–47.
31. Schumacher, R.S.; Johnson, R.H. Synoptic disturbances over the equatorial South China Sea and western maritime continent during boreal winter. *Monthly Weather Review* **2005**, *133*, 489–503.
32. Song, F.; Feng, Z.; Leung, L.R.; Pokharel, B.; Wang, S.Y.S.; Chen, X.; Sakaguchi, K.; Wang, C.c. Crucial Roles of Eastward Propagating Environments in the Summer MCS Initiation Over the U.S. Great Plains. *Journal of Geophysical Research: Atmospheres* **2021**, *126*, e2021JD034991, [https://agupubs.onlinelibrary.wiley.com/doi/pdf/10.1029/2021JD034991]. e2021JD034991 2021JD034991, doi:https://doi.org/10.1029/2021JD034991.
33. Saufina, E.; Trismidianto.; Risyanto.; Fathrio, I.; Harjupa, W. Impact of cross equatorial northerly surge (CENS) on Jakarta heavy rainfall and its interaction with tropical cyclone (Case study: 18-25 February 2020). *AIP Conference Proceedings* **2021**, *2366*, 050002, [https://aip.scitation.org/doi/pdf/10.1063/5.0059995]. doi:10.1063/5.0059995.
34. Hamada, J.I.; Mori, S.; Kubota, H.; Yamanaka, M.D.; Haryoko, U.; Lestari, S.; Sulistyowati, R.; Syamsudin, F. Interannual Rainfall Variability over Northwestern Jawa and its Relation to the Indian Ocean Dipole and El Niño-Southern Oscillation Events. *SOLA* **2012**, *8*, 69–72.
35. Nur'utami, M.N.; Hidayat, R. Influences of IOD and ENSO to Indonesian Rainfall Variability: Role of Atmosphere-ocean Interaction in the Indo-pacific Sector. *Procedia Environmental Sciences* **2016**, *33*, 196–203. The 2nd International Symposium on LAPAN-IPB Satellite (LISAT) for Food Security and Environmental Monitoring, doi:https://doi.org/10.1016/j.proenv.2016.03.070.
36. Baranowski, D.B.; Flatau, M.K.; Flatau, P.J.; Karnawati, D.; Barabasz, K.; Labuz, M.; Latos, B.; Schmidt, J.M.; Paski, J.A.I.; Marzuki. Social-media and newspaper reports reveal large-scale meteorological drivers of floods on Sumatra. *Nature Communications* **2020**, *11*, 2503. doi:10.1038/s41467-020-16171-2.